# PRELIMINARY STUDY TOWARD SURFACE TEXTURE AS A PROCESS SIGNATURE IN LASER POWDER BED FUSION ADDITIVE MANUFACTURING

**Jason C. Fox[1], Shawn P. Moylan[1], and Brandon M. Lane[1]**
**[1]Intelligent Systems Division**
**National Institute of Standards and Technology**
**Gaithersburg, MD 20899**

**ABSTRACT**
Additive manufacturing (AM) allows for highly complex designs that cannot be achieved through subtractive or formative manufacturing techniques. A limiting factor of AM, however, is the as-built surface quality. Additionally, there is limited knowledge on how specific surface features or defects translate to measured surface parameters. If a strong quantitative understanding of the relationships between the processes that cause specific surface features and the measured surface parameters can be developed, then surface texture has the potential to be developed as a process signature. Vertical and upward-facing surfaces of varying angles and process parameters were built and analyzed. Analysis of *Ra* was found to provide little information on the specific features that make up the surface texture. *RSm* and *Rc*, however, can indicate a shift between surfaces dominated by partially melted powder particles and ones dominated by material from the re-solidified melt track, which was also seen for downward-facing surfaces in prior work. The correlations presented are a step toward developing surface texture as a process signature for AM.

**INTRODUCTION**
Additive manufacturing (AM) has emerged as a key technology for production applications [1]. Laser powder bed fusion (L-PBF), a subset of AM, in particular has generated a great deal of interest. This is due to the fine focusing optics, layer thicknesses of 20 μm to 100 μm, and the powers and velocities over which the system operates allows for fine detail compared to other AM technologies [2].

Despite the advantages of AM, however, a limiting factor affecting widespread adoption is the as-built surface topography of finished parts. Methods exist to process surfaces *in situ* [3,4] or *ex situ* [5,6], but are limited, especially as design complexity increases [7]. Thus, improvements in the as-built surface texture has been cited as a key need [8].

Optimization of surface roughness has been the focus of several studies in AM research. Craeghs *et al.* used optical sensors to control melting, resulting in a reduction in top and overhanging surface roughness [9]. Diatlov *et al.* performed a spectral analysis of the arithmetical mean roughness (*Ra*) for a wide range of surface slopes, finding a potential to determine surface characteristics [10]. Work by Abd-Elghany and Bourell investigated the effect of layer thickness on top and side surface roughness, finding that thick layers lead to increased surface roughness due to a tendency of the particles to form voids once removed during post processing [11]. Jamshidinia and Kovacevic found that an increase in surface roughness can occur due to increased heat accumulation causing an increase in partially melted powder particle attachment [12].

There is a wide range of mechanisms that contribute to the roughness of an AM surface, which include the process input parameters as well as the complex physical processes that occur during melting and solidification of the metal powder [13]. For example, Kleszczynski *et al.* found that there is a positional dependency on surface roughness [14], a factor commonly overlooked by the research community. Additionally, the majority of research cites *Ra* when determining surface roughness; however, this parameter tells us very little about the makeup of the surface. Some research has investigated additional parameters. For example, Triantaphyllou *et al.* found that the area skewness (*Ssk)* can be used to differentiate between upward- and downward-facing surfaces [15]. However, if surface texture is to be used as a process signature a strong quantitative understanding of the relationship between the mechanisms that contribute to surface texture and measured surface parameters, including and not limited to *Ra*, must be investigated and understood.

Related work by the authors has shown the potential of using existing parameters beyond *Ra* to better understand the characteristics of a surface for downward-facing surfaces [16]. In this work, upward-facing and vertical surfaces of the parallelepipeds are analyzed. Qualitative and quantitative analyses show that relationships seen in the mean spacing of profile irregularities (*RSm*) and the mean height of the profile elements (*Rc*) of downward-facing surfaces can also be seen in the vertical and upward-facing surfaces. These correlations point toward a direction for further research into relating surface finish metrics with the physics of the laser powder bed fusion process and the development of surface texture as a process signature.

## EXPERIMENTAL PROCEDURE

The experiments focus on test parts that were built on a commercially available L-PBF system. The parts were designed as symmetrical parallelepipeds, having two parallel, vertical parallelogram faces; two rectangular faces; and two square faces. The acute angle of the parallelogram was varied, resulting in test parts with inclined/overhang angles (α) of 30˚, 45˚, 60˚, and 75˚ as measured from the build plane. Figure 1 illustrates the test part with α=60˚.

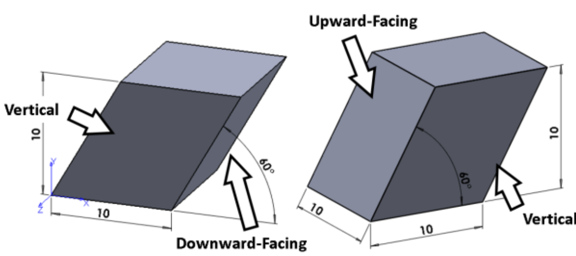


*FIGURE 1. Model parallelepiped for surface characterization, where α=60°. Dimensions are in millimeters. Build direction is positive z.*

The test parts were built on the EOS M270[1] system at the National Institute of Standards and Technology (NIST). All parts were fabricated in the same build. Stainless steel powder (EOS GP1, which is chemically equivalent to U.S. classification 17-4 stainless steel) reclaimed from several previous builds was used. The powder was screened through an 80 µm sieve before the build. Since it is likely that the condition of the feedstock powder affects the surface texture of the resulting part, powder samples were taken and are currently being analyzed.

Prior work assessed the effect of process parameters on surface characteristics for downward-facing surfaces [16]. In that work, contour parameters with varying laser beam power and travel velocity were chosen in order to cover a wide range of the process space. It was found that two sets of parameters led to highly different surface characteristics. As such, the focus of this work will be on Characterizing the vertical and upward-facing surfaces from the two contour parameters sets shown in TABLE 1.

*TABLE 1. Process parameters for experiments. Contour numbers are chosen to match designations from prior work* [16].

| Contour Number | Power (W) | Velocity (mm/s) | Line Energy – *P/v* (J/m) |
|---|---|---|---|
| 4 | 40 | 700 | 57.1 |
| 9 | 195 | 700 | 278.6 |

A total of eight parallelepipeds were analyzed (i.e., two contour parameter sets with four values of α). As such, eight upward-facing surfaces and 16 vertical surfaces were analyzed (since each parallelepiped has two vertical surfaces). Test parts were positioned equidistant from the center of the build platform with the downward-facing surface of the parallelepiped forming a straight line to the center of the laser source. This was done to prevent as many of the positional dependency issues seen by Kleszczynski *et al.* [14] as possible. All surfaces were also at a slight angle (i.e., not parallel) to the recoater blade and that angle varies based on position on the build plate to maintain a constant angle relative to the laser. Additionally, the vertical surfaces are either facing towards the center of the plate (labeled Towards in later figures) or away from the center of the plate (labeled Away).

[1] Certain commercial entities, equipment, or materials may be identified in this document in order to describe an experimental procedure or concept adequately. Such identification is not intended to imply recommendation or endorsement by the National Institute of Standards and Technology, nor is it intended to imply that the entities, materials, or equipment are necessarily the best available for the purpose.

## ANALYSIS METHODS

Surface characterization was performed using a white light interferometer, described in detail in [17], and 10x objective lens. Using white light interferometry to analyze a very rough surface is a challenge due to difficulty in achieving null fringe condition (perfect leveling of the sample surface being measured). Because of this, a diamond-turned aluminum disk was first used to level the sample platform prior to any measurements. Thus, the best leveling possible, assuming that the surface being measured and the surface laying on the platform are parallel, was achieved. This leveling procedure was performed before each measurement session to maintain a consistent leveling for each sample and prevent deviations due to errors caused by the leveling of the samples.

Seven images with 20 percent overlap were taken along each surface (perpendicular to the layers) and stitched together to create an approximately 5 mm long measurement. This created a large enough measurement of the sample surface to properly perform digital Gaussian filtering based on the ISO 4287 standard [18]. The values presented used a bandpass digital Gaussian filter with a short cut-off length of 25 μm and a long cut-off length of 0.8 mm. The filtering process results in an evaluation length equal to five long cut-off lengths, or 4 mm. These filters are defined by ISO 4287 and represent a common practice in AM surface roughness research [19].

Qualitative analysis using scanning electron microscopy was performed on selected surfaces.

## RESULTS

### <u>Qualitative Analysis</u>

Scanning electron microscope (SEM) images for two vertical surfaces can be seen in FIGURE 2. FIGURE 2a) shows a vertical surface built with set 4. In this image, the surface is dominated by partially melted powder particles, but the re-solidified material from the melt track as well as gaps in the melt surface can be seen.

FIGURE 2b) shows a vertical surface built with set 9. In this image, fewer partially melted particles are present and the surface is dominated by the re-solidified material from the melt track. Additionally, this combination of power and velocity led to material that was damaged by the recoater blade on the downward-facing surface [16]. Similar damage can also be seen in this figure. A key difference between the vertical surface and the downward-facing surface, however, is the nature of the damaged material. These surfaces have a different orientation relative to the recoater blade because they form 90° angle when viewed from above. As such, the damaged material is scraped into the part from the vertical surface and out of the part from the downward-facing surface.

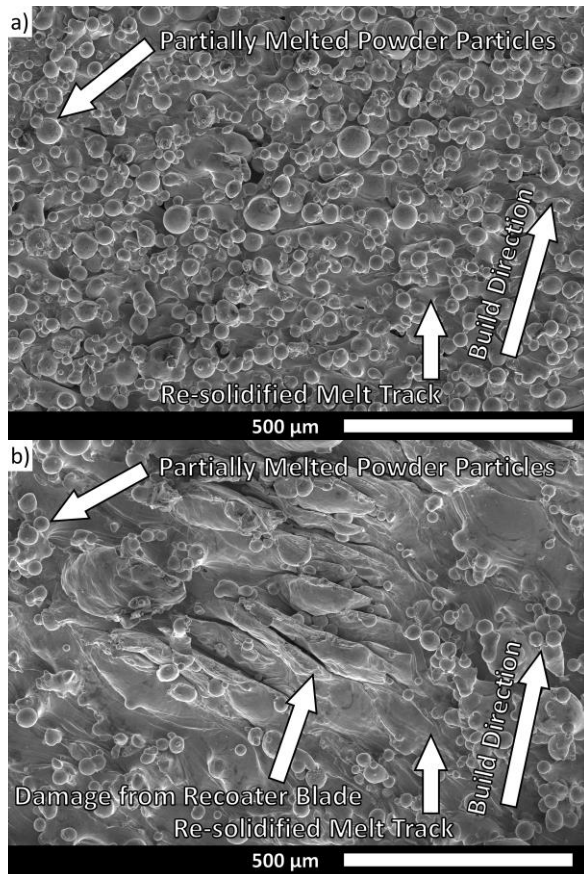


*FIGURE 2. Vertical surfaces built with a) set 4 and b) set 9.*

SEM images for two upward-facing surfaces can be seen in FIGURE 3. FIGURE 3a) shows the upward-facing surface built with set 4. Similar to the vertical surface with the same set, this surface is dominated by partially melted powder particles but the re-solidified material from the melt track as well as gaps in the melt surface can be seen.

FIGURE 3b) shows the upward-facing surface built with set 9. This surface is dominated by the re-solidified material from the melt track with very few partially melted powder particles. There is no deformation of material that was seen in the vertical and downward-facing surfaces. Additionally, there is little evidence of the layers or of any stair-stepping phenomenon commonly associated with AM.

It is interesting to note that vertical, upward-facing, and downward-facing surfaces built with set 4 are all very similar qualitatively. The selection of this parameter set for the contours would make sense for a manufacturer if having a consistent exterior surface, regardless of position or orientation, is the desirable outcome.

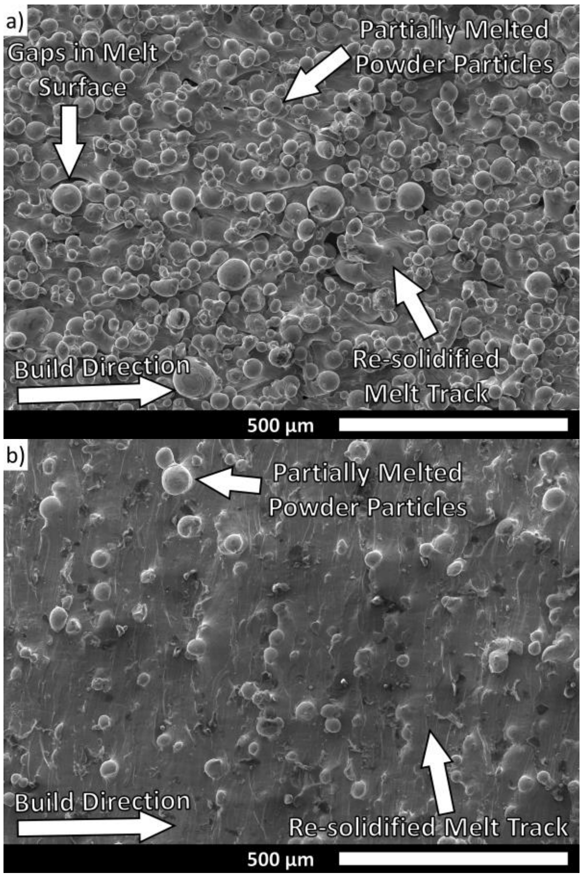


*FIGURE 3. Upward-facing surfaces for α=60° built with a) set 4 and b) set 9.*

## Quantitative Analysis

### *Vertical Surface Analysis*

Analysis of *Ra* for the vertical surfaces can be seen in FIGURE 4. As mentioned previously, these parallelepipeds were built such that the downward-facing surface forms a straight line to the center of the plate. Therefore, the vertical surfaces are either facing towards the center of the plate (labeled Towards) or away from the center of the plate (labeled Away).

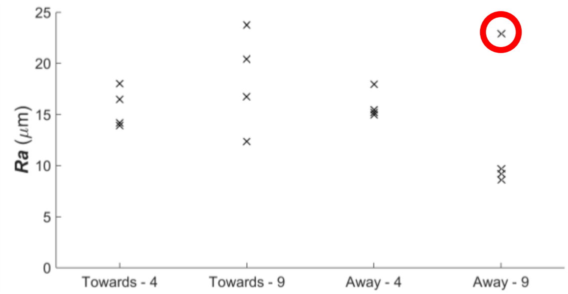


*FIGURE 4. Ra vs orientation relative to the center of the build platform and contour parameter set for the vertical surfaces. Outlier described in text is highlighted by a red circle.*

FIGURE 4 shows that it is difficult to develop a physical interpretation of the surface through *Ra* alone. An interesting observation, however, is that the high value outlier for the Vertical Away surface built with set 9 (highlighted by the red circle) could be due to the orientation relative to the recoater blade. Three of the vertical surfaces facing away from the center of the plate and built with parameter set 9 were oriented such that the recoater blade was going into the surface when spreading powder, while the outlier was oriented such that the recoater blade was coming out of the surface. Thus, the increase in surface roughness could be due to damaged material protruding from the surface and additional qualitative analysis is required to confirm.

Analysis of *Rc* and *RSm* for the vertical surfaces can be seen in FIGURE 5. Little variation can be seen in *Rc* and *RSm* for the parts built with set 4. For set 9, there is an increase in *RSm* when compared to set 4, which is expected from SEM images as the surface for set 9 is dominated less by partially melted powder particles and more by the re-solidified material from the melt track.

Another interesting finding is the difference in *Rc* for set 9 depending on whether the surface is facing towards or away from the center of the plate. This suggests that there is also a positional dependence in the *Rc* parameter, similar to what was seen by Kleszczynski *et al.* [14], but more qualitative analysis of the surfaces is required to determine the cause of this change.

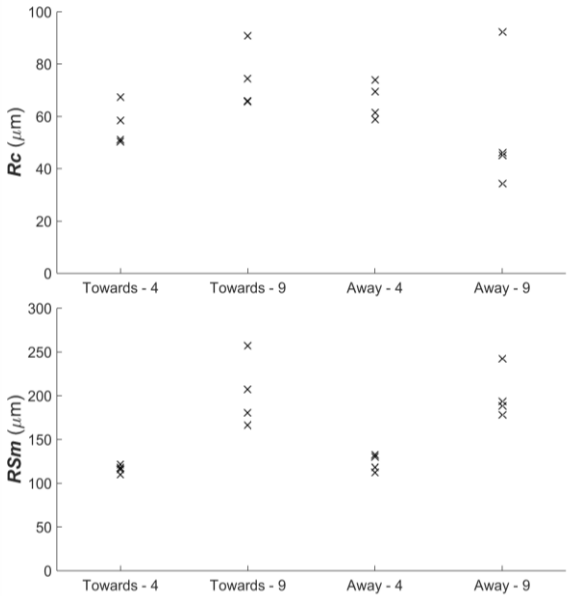


*FIGURE 5. Rc and RSm for the vertical surfaces.*

### *Upward-Facing Surface Analysis*

Analysis of *Ra* for the upward-facing surfaces as well as the downward-facing surfaces from prior work is presented in FIGURE 6 [16]. As was seen in the prior work, it can be difficult to discern differences in *Ra* from process parameters for the downward-facing surfaces. The upward-facing surfaces, however, exhibit a noticeable difference in *Ra*. Additionally, *Ra* for the upward-facing surfaces built with set 9 decreases as α decreases. This is likely due to the extremely small number of partially melted powder particles seen in SEM images, causing *Ra* to be dependent almost entirely on the re-solidified melt track.

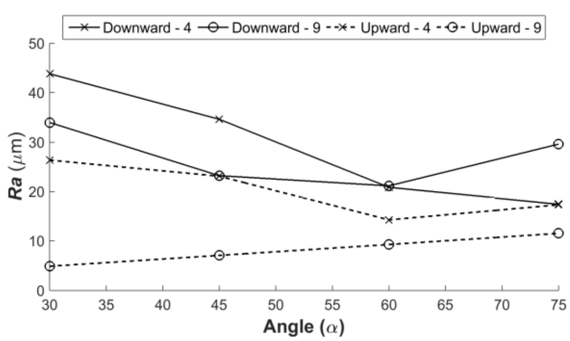


*FIGURE 6. Ra vs angle for downward- [16] and upward-facing surfaces.*

Analysis of *Rc* and *RSm* for the upward-facing surfaces as well as the downward-facing surfaces from prior work can be seen in FIGURE 7 [16]. As expected, *Rc* decreases and *RSm* increases as we move from surfaces dominated by partially melted powder particles to ones dominated by the re-solidified melt track.

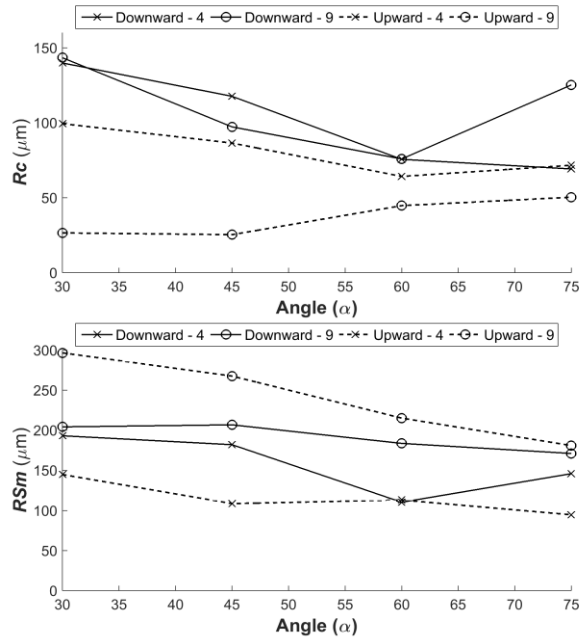


*FIGURE 7. Rc and RSm vs angle for downward- [16] and upward-facing surfaces.*

## CONCLUSIONS

Analysis of upward-facing surfaces of 30°, 45°, 60°, and 75° relative to the build platform and vertical surfaces (90° relative to the build platform) was performed qualitatively by SEM and quantitatively by white light interferometry. Samples were built with two power and velocity combinations, which were found by prior work to create drastic changes in the surface features for downward-facing surfaces [16]. As with the downward-facing surfaces, *Ra* was shown to provide little insight into characteristics of the vertical and upward-facing surface. *Rc* and *RSm* for the vertical and upward-facing surfaces, however, showed similar correlations to the downward-facing surfaces where *Rc* increases and *RSm* decreases as surfaces change from being dominated by the re-solidified melt track to those dominated by the partially melted powder particles. While additional experiments and analysis are required to match specific surface features with the physical process of L-PBF, these correlations provide insight into the use of surface texture as a process signature.

**ACKNOWLEGEMENTS**
The authors would like to thank Dr. Mark Stoudt and Dr. Maureen Williams of NIST for their assistance with the SEM analyses.

**REFERENCES**

[1] Taminger KM, Hafley RA. Electron beam freeform fabrication for cost effective near-net shape manufacturing. NATO/RTO AVT-139 Specialists' Meeting on Cost Effective Manufacture via Net Shape Processing, vol. AVT-139, Amsterdam, The Netherlands: 2006, p. 9–25.

[2] Yadroitsev I. Selective laser melting: direct manufacturing of 3D-objects by selective laser melting of metal powders. Saarbrücken: Lambert Acad. Publ; 2009.

[3] Yasa E, Kruth J-P, Deckers J. Manufacturing by combining Selective Laser Melting and Selective Laser Erosion/laser re-melting. CIRP Annals - Manufacturing Technology 2011;60:263–6. doi:10.1016/j.cirp.2011.03.063.

[4] Mumtaz KA, Hopkinson N. Selective Laser Melting of thin wall parts using pulse shaping. Journal of Materials Processing Technology 2010;210:279–87. doi:10.1016/j.jmatprotec.2009.09.011.

[5] Liu X, Chu PK, Ding C. Surface modification of titanium, titanium alloys, and related materials for biomedical applications. Materials Science and Engineering: R: Reports 2004;47:49–121. doi:10.1016/j.mser.2004.11.001.

[6] Lane BM, Moylan SP, Whitenton EP. Post-Process Machining of Additive Manufactured Stainless Steel. Proceedings of the 2015 ASPE Spring Topical Meeting: Achieving Precision Tolerances in Additive Manufacturing, Raleigh, NC: ASPE; 2015.

[7] Pyka G, Burakowski A, Kerckhofs G, Moesen M, Van Bael S, Schrooten J, et al. Surface modification of Ti6Al4V open porous structures produced by additive manufacturing. Advanced Engineering Materials 2012;14:363–70. doi:10.1002/adem.201100344.

[8] Measurement Science Roadmap for Metal-Based Additive Manufacturing, Gaithersburg, MD: NIST; 2012.

[9] Craeghs T, Bechmann F, Berumen S, Kruth J-P. Feedback control of Layerwise Laser Melting using optical sensors. Physics Procedia 2010;5, Part B:505–14. doi:10.1016/j.phpro.2010.08.078.

[10] Diatlov A, Buchbinder D, Meiners W, Wissenbach K, Bultmann J. Towards surface topography: Quantification of Selective Laser Melting (SLM) built parts. Innovative Developments in Virtual and Physical Prototyping: Proceedings of the 5th International Conference on Advanced Research in Virtual and Rapid Prototyping, Leiria, Portugal: 2012, p. 595–602.

[11] Abd-Elghany, K, Bourell, DL. Property evaluation of 304L stainless steel fabricated by selective laser melting. Rapid Prototyping Journal 2012;18:420–8. doi:10.1108/13552541211250418.

[12] Jamshidinia M, Kovacevic R. The influence of heat accumulation on the surface roughness in powder-bed additive manufacturing. Surf Topogr: Metrol Prop 2015;3:14003. doi:10.1088/2051-672X/3/1/014003.

[13] Taylor JS. Physical processes linking input parameters and surface morphology in additive manufacturing. 2015 ASPE Spring Topical Meeting: Achieving Precision Tolerances in Additive Manufacturing, Raleigh, NC: ASPE; 2015, p. 70–1.

[14] Kleszczynski S, Ladewig A, Friedberger K, zur Jacobsmühlen J, Merhof D, Witt G. Position Dependency of Surface Roughness in Parts from Laser Beam Melting Systems. Solid Freeform Fabrication Symposium, Austin, TX: 2015.

[15] Triantaphyllou A, Giusca CL, Macaulay GD, Roerig F, Hoebel M, Leach RK, et al. Surface texture measurement for additive manufacturing. Surf Topogr: Metrol Prop 2015;3:24002. doi:10.1088/2051-672X/3/2/024002.

[16] Fox JC, Moylan SP, Lane BM. Effect of process parameters on the surface roughness of overhanging structures in laser powder bed fusion additive manufacturing. Procedia CIRP, Charlotte, NC: 2016. doi:10.1016/j.procir.2016.02.347.

[17] Leach RK, editor. Fundamental Principles of Engineering Nanometrology. Oxford: William Andrew Publishing; 2010.

[18] ISO 4287:1997. Geometrical Product Specifications (GPS) – Surface texture: Profile method – Terms, definitions and surface texture parameters. ISO, Geneva 1997.

[19] Petzing J, Coupland J, Leach RK. The Measurement of Rough Surface Topography using Coherence Scanning Interferometry. National Physical Laboratory Good Practice Guide No. 116, Teddington, UK: 2010.